Three-Dimensional Laminar Boundary Layers with Large Cross-Flow

R. VAGLIO-LAURIN* AND G. MILLER†
New York University, Bronx, New York

The paper is concerned with the detailed formulation and evaluation of a previously proposed physical model and method of analysis for three-dimensional hypersonic laminar boundary layers. In this approach, the boundary layer is subdivided into two (inner and outer) regions characterized by widely different momentum fluxes per unit area. The subdivision leads to considerable simplifications in the statements of the inner and outer equations and in the determination of the associated solutions. An over-all description of the flow is obtained by matching the two solutions. The heuristic model and method of analysis are corroborated by comparing their predictions with those of "exact" numerical solutions of the complete boundary-layer equations. The family of self-preserving flows near a plane of symmetry is used as test problem. The two-layer model yields closed-form results for velocity and enthalpy profiles as well as for skin friction and wall heat transfer, in good agreement with the exact predictions. The application of the model to general three-dimensional flows is discussed in the context of this comparison and of the salient features of the analysis; inter-alia, the extension to moderate Mach number flows is indicated.

1. Introduction

RECENT theoretical studies of compressible and, in particular hypersonic, three-dimensional laminar boundary layers can broadly be divided into two categories, namely a) those devoted to specific classes of flows amenable to simplified description and analysis, e.g., similar solutions,[1,2] negligible[3,4] and small[5,6] cross-flow approximations and b) those concerned with fully numerical solutions.[7] The studies in category a have provided much useful information and understanding on the behavior of three-dimensional flows; however, their range of applicability in general situations remains uncertain. The studies in category b possess general applicability, in principle; however, they essentially represent numerical experiments which must rely on separate physical-analytical models for a comprehensive interpretation and a coordinated understanding of the results.

An alternative approach to general three-dimensional problems consists in seeking approximations that are intimately related to the physical characteristics of the flow, at least for specific broad ranges of flight velocities and configurations. In this vein, a simplified physical and analytical model was set forth in Ref. 8 for hypersonic flows. The model recognizes two regions; 1) a thin outer region where the fluid velocity and stagnation enthalpy are nearly the same as those in the external inviscid flow, the density is comparable to the external density, the cross-flow is negligible, and the possibly nonsimilar flow is described by *linear* partial differential equations and 2) an inner region, comprising the major portion of the boundary layer, where the cross-flow can be appreciable, but the inertial forces are small compared to the pressure and viscous forces, and the flow is locally similar, viz. governed by ordinary differential equations.

Received June 6, 1969; presented as Paper 69-710 at the AIAA Fluid and Plasma Dynamics Conference, San Francisco, Calif., June 16–18, 1969; revision received March 31, 1970. This paper is based on research sponsored by the United States Air Force Office of Scientific Research (OAR) under Grant AF-AFOSR-68-1551.

* Professor of Aeronautics and Astronautics. Associate Fellow AIAA.

† Assistant Professor of Aeronautics and Astronautics. Member AIAA.

The subdivision of the boundary layer into two regions has been used previously with success in analyses of two-dimensional flows at low as well as high velocities. These analyses may be categorized in two groups; a) the analyses where the two layer approach is justified by asymptotic considerations associated with the presence of a large parameter in the governing equations (e.g., the transverse curvature parameter in the equations describing the axial viscous flow over a long circular cylinder[9] and the strong interaction region over a slender cone at zero incidence[10]), and b) the analyses where the two layer model is justified by heuristic physical arguments instead of rigorous asymptotic considerations (e.g., the Von Karman-Millikan[11] and Stratford[11] investigations of flows in adverse pressure gradients). Although not rigorous, the studies of group b have performed a useful role in demonstrating the dominant contributions to dynamic equilibrium in different regions of the boundary layer, and in providing reasonably accurate results by relatively rapid calculations.

The analysis presented in this paper is conceptually in the vein of group b. Attention is focused on flows in the presence of favorable pressure gradients and of moderate adverse pressure gradients which do not produce separation in either the streamwise or the cross-flow direction. The heuristic two region model for these classes of hypersonic three-dimensional boundary layers[8] is examined with a view toward the analytical implementation of the related method of analysis, toward the assessment of the solutions obtained by this method in comparison with "exact" numerical results, and toward the possible application of the model outside the range of hypersonic conditions. The general statement of the problem, including an approach to the systematic matching of inner and outer solutions, is presented first (sec. 2). The analysis is then specialized to a class of hypersonic laminar flows near a plane of symmetry,[2] which are chosen as test case for demonstrating and assessing the proposed approach. Closed form solutions valid in the outer region (Sec. 3) and in the inner region (Sec. 4) are obtained and matched to provide a complete description of the flow (Sec. 5). The accuracy of the two layer analysis is demonstrated by comparing the present results with those of Ref. 2 (Sec. 6). Finally the applicability of the model under nonhypersonic conditions, as well as its implications for the proper formulation of fully numerical solutions and for the use of integral methods, are discussed.

2. Statement of the Problem

It is well known[12] that hypersonic laminar boundary layers exhibit the following characteristics (Fig. 1): 1) a thin outer region, adjacent to the edge, where the density and the momentum flux per unit area rapidly decrease from their inviscid stream values, while the velocity and the stagnation enthalpy remain essentially undisturbed; and 2) an inner region, which encompasses the major portion of the boundary layer, where the local density and momentum flux per unit area are much smaller than their counterparts in the inviscid stream. These features readily suggest a physical model for three-dimensional flows. In a system of orthogonal curvilinear coordinates (x_1,x_2,x_3) having the surface $x_3 = 0$ coincident with the body surface, and the lines (x_2 = constant, $x_3 = 0$) coincident with the streamlines of the inviscid flow (Fig. 2), the high density outer fluid layer plays the role of an equivalent solid plate with respect to the low density inner layer. The outer layer, moving parallel to the surface of the body at the inviscid flow velocity v_{1e} (v_i denotes the x_i-component of velocity, a subscript e denotes properties of the inviscid flow) develops negligible cross-flow (relative to the inviscid streamlines) because it possesses momentum comparable to that of the freestream. The inner layer is dragged by the outer one; its state of motion is determined by the combined action of the equivalent outer plate, of the actual wall, and of the streamwise $(\partial p/\partial x_1)$ and transversal $(\partial p/\partial x_2)$ pressure gradients. Because of low density and inertia, this motion (of the inner layer) is dominated by viscous and pressure forces and, therefore, is Couette-like in the direction of the external flow and Poiseuille-like in the direction transversal thereto.

Consistent with the considerations above, simplified sets of equations appropriate to the inner and outer regions were suggested in Ref. 8, where it was also indicated that matching of the inner and outer solutions would provide a complete description of the flow. These suggestions are elaborated in quantitative fashion below. The discussion is based on a description of the flow in curvilinear streamline coordinates x_i (i = 1, 2, 3) which clearly manifest the influence of the cross-flow and its derivatives upon the inner and outer solutions, as well as the zones of dependence and/or influence[7] to be considered in numerical solutions of the problem.

In curvilinear streamline coordinates, with metric elements e_i, the boundary-layer equations for a perfect gas with unit Prandtl number take the form

$$(\partial/\partial x_1)(e_2e_3\rho v_1) + (\partial/\partial x_2)(e_1e_3\rho v_2) + (\partial/\partial x_3)(e_1e_2\rho v_3) = 0 \quad (1)$$

$$\rho\left[\frac{Dv_1}{Dt} + v_1v_2\frac{\partial e_1}{e_1e_2\partial x_2} - v_2^2\frac{\partial e_2}{e_2e_1\partial x_1}\right] = -\frac{\partial p}{e_1\partial x_1} + \frac{\partial}{e_3\partial x_3}\left(\mu\frac{\partial v_1}{e_3\partial x_3}\right) \quad (2)$$

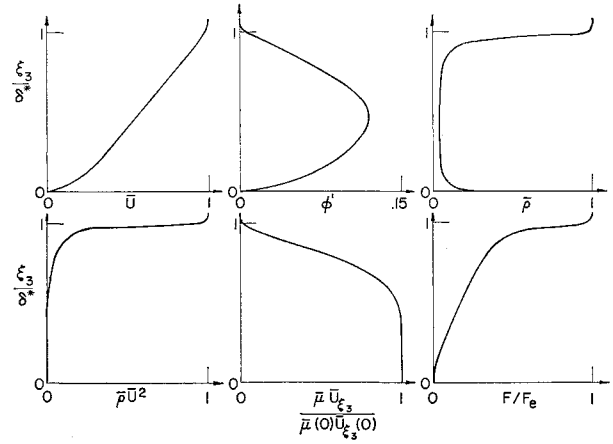

Fig. 1 Typical profiles for a three-dimensional hypersonic laminar boundary layer near a plane of symmetry.

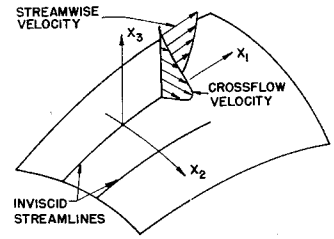

Fig. 2 Schematic diagram of orthogonal curvilinear coordinate system.

$$\rho\left[\frac{Dv_2}{Dt} + v_1v_2\frac{\partial e_2}{e_2e_1\partial x_1} - v_1^2\frac{\partial e_1}{e_1e_2\partial x_2}\right] = -\frac{\partial p}{e_2\partial x_2} + \frac{\partial}{e_3\partial x_3}\left(\mu\frac{\partial v_2}{e_3\partial x_3}\right) \quad (3)$$

$$\rho(DH/Dt) = (\partial/e_3\partial x_3)[\mu(\partial H/e_3\partial x_3)] \quad (4)$$

where

$$D/Dt = v_i(\partial/e_i\partial x_i) \quad (i = 1,2,3) \quad (5)$$

v_i denotes the x_i-component of velocity, ρ the density, μ the viscosity, and H the stagnation enthalpy. Associated with these equations are the boundary conditions (for an impermeable wall)

$$x_3 = 0, \quad v_i = 0, H = H_w \quad (6a)$$

$$x_3 \to \infty, \quad v_1 \to v_{1e}, v_2 \to 0, \quad H \to H_e \quad (6b)$$

For present purposes, it is useful to recast the Eqs. (1–4) in terms of Levy-Lees-like (except for the density transformation) independent and dependent variables. With the independent variables and metric elements

$$\xi_1 = \int_0^{x_1} \rho^*\mu^*v_1^*e_2^{*2}e_1^*dx_1, \quad \xi_2 = x_2, \quad \xi_3 = \frac{\rho^*v_1^*e_2^*e_3^*x_3}{(2\xi_1)^{1/2}} \quad (7a)$$

$$\bar{e}_i = e_i/e_i^*$$

where ρ^*, μ^*, etc. denote inviscid flow properties on a selected edge streamline ($x_2 = x_2^*$, $x_3 = 0$), and with the dependent variables

$$\bar{v}_1 = v_1/v_1^*, \quad \bar{v}_2 = v_2/v_1^*$$

$$\bar{v}_3 = (2\xi_1)^{1/2}\left[\frac{v_3}{e_2^*v_1^*\mu^*} - \rho^*e_2^*e_3^*v_1\left(\frac{\partial x_3}{\partial\xi_1} - \frac{x_3}{2\xi_1}\right)\frac{\bar{e}_3}{\bar{e}_1}\right] \quad (7b)$$

$$\bar{H} = (H - H_w)/(H_e - H_w), \quad \bar{\rho} = \rho/\rho^*, \quad \bar{\mu} = \mu/\mu^*$$

the governing equations become

$$2\xi_1(\partial/\partial\xi_1)(\bar{e}_2\bar{e}_3\bar{\rho}\bar{v}_1) + (\partial/\partial\xi_2)(\bar{e}_1\bar{e}_3\alpha^*\bar{\rho}\bar{v}_2) + (\partial/\partial\xi_3)(\bar{e}_1\bar{e}_2\bar{\rho}\bar{v}_3) - \xi_3(\partial/\partial\xi_3)(\bar{e}_2\bar{e}_3\bar{\rho}\bar{v}_1) = 0 \quad (8)$$

$$\bar{\rho}\frac{\bar{D}\bar{v}_1}{Dt} + \bar{\rho}\omega\bar{v}_1\bar{v}_2 + \frac{\beta^*}{\bar{e}_1}\bar{\rho}\bar{v}_1^2 = -\frac{\beta^*}{\bar{e}_1\rho^*v_1^*}\frac{(\partial p/\partial\xi_1)}{(\partial v_1^*/\partial\xi_1)} + \frac{\partial}{\bar{e}_3\partial\xi_3}\left(\bar{\mu}\frac{\partial\bar{v}_1}{\bar{e}_3\partial\xi_3}\right) \quad (9)$$

$$\bar{\rho}\frac{\bar{D}\bar{v}_2}{Dt} - \bar{\rho}\omega\bar{v}_1^2 + \frac{\beta^*}{\bar{e}_1}\bar{\rho}\bar{v}_1\bar{v}_2 = -\frac{\beta^*}{\bar{e}_2\rho^*v_1^*}\left(\frac{\alpha^*}{2\xi_1}\right)\frac{(\partial p/\partial\xi_2)}{(\partial v_1^*/\partial\xi_1)} + \frac{\partial}{\bar{e}_3\partial\xi_3}\left(\bar{\mu}\frac{\partial\bar{v}_2}{\bar{e}_3\partial\xi_3}\right) \quad (10)$$

$$\bar{\rho}(\bar{D}\bar{H}/Dt) = (\partial/\bar{e}_3\partial\xi_3)[\bar{\mu}(\partial\bar{H}/\bar{e}_3\partial\xi_3)] \quad (11)$$

with

$$\bar{\rho} = \frac{\rho_e}{\rho^*}\left[1 - m\left(\frac{v_{1e}^2}{v_1^{*2}}\right)\right]\Big/\left[\frac{H_w}{H_e} + \left(1 - \frac{H_w}{H_e}\right)\bar{H} - m(\bar{v}_1^2 + \bar{v}_2^2)\right] \quad (12a)$$

$$m = v_1^{*2}/(2H_e) \tag{12b}$$

$$\frac{\bar{D}}{Dt} = 2\xi_1\bar{v}_1\frac{\partial}{\bar{e}_1\partial\xi_1} + \alpha^*\bar{v}_2\frac{\partial}{\bar{e}_2\partial\xi_2} + \left(\bar{v}_3 - \xi_3\bar{v}_1\frac{\bar{e}_3}{\bar{e}_1}\right)\frac{\partial}{\bar{e}_3\partial\xi_3} \tag{12c}$$

$$\omega = \alpha^*\frac{\partial\bar{e}_1}{\bar{e}_1\bar{e}_2\partial\xi_2} - \frac{\bar{v}_2}{\bar{v}_1}\left(\frac{2\xi_1}{\bar{e}_1}\right)\left(\frac{\partial\bar{e}_2}{\bar{e}_2\partial\xi_1} + \frac{\partial e_2^*}{e_2^*\partial\xi_1}\right) \tag{12d}$$

$$\alpha^* = (2\xi_1)/(\rho^*\mu^*v_1^*e_2^{*3}) \tag{12e}$$

$$\beta^* = (2\xi_1/v_1^*)(\partial v_1^*/\partial\xi_1) \tag{12f}$$

The boundary conditions associated with Eqs. (8–11) are

$$\xi_3 = 0, \quad \bar{v}_i = \bar{H} = 0 \tag{13a}$$

$$\xi_3 \to \infty, \quad \bar{v}_1 \to (v_{1e}/v_1^*) = \bar{v}_{1e}, \quad \bar{v}_2 \to 0, \quad \bar{H} \to 1 \tag{13b}$$

The continuity Eq. (8) can be satisfied identically by introducing two stream functions $(2\xi_1)^{1/2}F(\xi_i)$ and $(2\xi_1)^{1/2}\varphi(\xi_i)$ such that

$$\begin{gathered}\partial F/\partial\xi_3 = \bar{e}_2\bar{e}_3\bar{\rho}\bar{v}_1, \quad \partial\varphi/\partial\xi_3 = (\alpha^*/2\xi_1)\bar{e}_1\bar{e}_3\bar{\rho}\bar{v}_2 \\ F + 2\xi_1\left(\frac{\partial F}{\partial\xi_1} - \frac{\xi_3}{2\xi_1}\frac{\partial F}{\partial\xi_3} + \frac{\partial\varphi}{\partial\xi_2}\right) = -\bar{e}_1\bar{e}_2\bar{\rho}\bar{v}_3\end{gathered} \tag{14}$$

Examination of the Eqs. (8–11) readily yields the two layer behavior for hypersonic boundary layers, wherein $m \to 1$, $\bar{\rho} \to 0$, except for $\{(H_w/H_e) + [1 - (H_w/H_e)]\bar{H} - m[\bar{v}_1^2 + \bar{v}_2^2]\} = 0(1 - m)$, and the characteristic thickness δ^*, e.g., the displacement thickness, becomes $0[(1 - m)^{-1}]$. In accord with the behavior previously exhibited in Fig. 1, the outer region is characterized by‡

$$\begin{gathered}(\xi_3 - \delta^*) = 0(1), \ \bar{\rho} = (\bar{\rho}_e\bar{\mu}_e)/\bar{\mu} = 0(1) \\ F = 0(1), \ \varphi \approx \text{const} = 0(1) \\ V_1 = (\bar{v}_{1e} - \bar{v}_1) = 0(1 - m), \ V_2 = -\bar{v}_2 = 0(1 - m) \\ V_3 = \bar{v}_3 = 0(1), \ H_0 = (1 - \bar{H}) = 0(1 - m) \\ \frac{\partial}{\partial\xi_3}[F,\bar{\rho},\bar{\mu}] = 0(1), \quad \frac{\partial}{\partial\xi_3}[\varphi,\bar{H},\bar{v}_1,\bar{v}_2] = 0(1 - m) \\ (\partial^2/\partial\xi_3^2)[\bar{H},\bar{v}_1,\bar{v}_2] = 0(1 - m)\end{gathered} \tag{15}$$

the inner region (for flows not approaching separation) is characterized by

$$\begin{gathered}\xi_3 = 0(1), \ \bar{\rho} = (\bar{\rho}_e\bar{\mu}_e)/\bar{\mu} = 0(1 - m) \\ F = 0[(1 - m)^2], \ \varphi = 0[(1 - m)^2] \\ V_1 = \bar{v}_{1e} - 0(1 - m), \ V_2 = 0(1 - m) \\ V_3 = 0(1 - m), \ H_0 = 1 - 0(1 - m) \\ \frac{\partial}{\partial\xi_3}[\bar{H},\bar{v}_1,\bar{v}_2] = 0(1 - m), \ \frac{\partial}{\partial\xi_3}[F,\varphi,\bar{\rho}] = 0[(1 - m)^2] \\ (\partial^2/\partial\xi_3^2)[\bar{H},\bar{v}_1,\bar{v}_2] = 0[(1 - m)^2]\end{gathered} \tag{16}$$

and the external flow by

$$\alpha^* = 0(1), \ \beta^* = 0(1 - m) \tag{17}$$

Simplified statements of Eqs. (8–11) appropriate to the inner and outer regions are obtained upon an order of magnitude analysis consistent with the estimates (15) and (16). If only the leading terms are retained, the inner equations are

$$(\partial/\bar{e}_3\partial\xi_3)[\bar{\mu}(\partial V_1/\bar{e}_3\partial\xi_3)] = -(\beta^*/\bar{e}_1\rho^*v_1^*)[(\partial p/\partial\xi_1)/(\partial v_1^*/\partial\xi_1)] \tag{18}$$

$$(\partial/\bar{e}_3\partial\xi_3)[\bar{\mu}(\partial V_2/\bar{e}_3\partial\xi_3)] = -(\beta^*\alpha^*/2\xi_1\bar{e}_2\rho^*v_1^*)(\partial p/\partial\xi_2)/(\partial v_1^*/\partial\xi_1) \tag{19}$$

$$(\partial/\bar{e}_3\partial\xi_3)[\bar{\mu}(\partial H_0/\bar{e}_3\partial\xi_3)] = 0 \tag{20}$$

viz. ordinary differential equations. To the same approximation the outer equations are reduced to linear partial differential equations

$$\frac{D_FV_1}{Dt} = \left(\frac{\bar{v}_{1e}^2}{\bar{e}_1}\right)\left(\beta^* + 2\frac{\partial\ln\bar{v}_{1e}}{\partial\ln\xi_1}\right) + \left(\frac{\beta^*}{\bar{e}_1\bar{\rho}}\right)\times\left(\frac{1}{\rho^*v_1^*}\right)\frac{(\partial p/\partial\xi_1)}{(\partial v_1^*/\partial\xi_1)} + \bar{e}_2^2\bar{\rho}_e\bar{\mu}_e\bar{v}_{1e}^2\left(\frac{\partial^2V_1}{\partial F^2}\right) \tag{21}$$

$$\frac{D_FV_2}{Dt} = -\left(\frac{\alpha^*\bar{v}_{1e}^2}{\bar{e}_1}\right)\left(\frac{\partial\bar{e}_1}{\bar{e}_2\partial\xi_2}\right) + \left(\frac{\beta^*\alpha^*}{2\xi_1\bar{e}_2\bar{\rho}}\right)\times\left(\frac{1}{\rho^*v_1^*}\right)\frac{(\partial p/\partial\xi_2)}{(\partial v_1^*/\partial\xi_1)} + \bar{e}_2^2\bar{\rho}_e\bar{\mu}_e\bar{v}_{1e}^2\left(\frac{\partial^2V_2}{\partial F^2}\right) - 2\xi_1\frac{\bar{v}_{1e}}{\bar{e}_1}\left\{\frac{\partial e_2^*}{e_2^*\partial\xi_1} + \frac{\partial\bar{e}_2}{\bar{e}_2\partial\xi_1}\right\}V_2 \tag{22}$$

$$D_FH_0/Dt = \bar{e}_2^2\bar{\rho}_e\bar{\mu}_e\bar{v}_{1e}^2(\partial^2H_0/\partial F^2) \tag{23}$$

where

$$D_F/Dt = (\bar{v}_{1e}/\bar{e}_1)\{2\xi_1(\partial/\partial\xi_1) - [F + 2\xi_1(\partial\varphi/\partial\xi_2)]\partial/\partial F\} \tag{24}$$

upon change of independent variables from (ξ_1,ξ_2,ξ_3) to (ξ_1,ξ_2,F) and use of Eq. (14) in the reduced form appropriate to the outer region.

$$\begin{gathered}(\partial F/\partial\xi_3) = \bar{e}_2\bar{e}_3\bar{\rho}\bar{v}_{1e} \\ F + 2\xi_1[(\partial F/\partial\xi_1) - (\xi_3/2\xi_1)(\partial F/\partial\xi_3) + (\partial\varphi/\partial\xi_2)] = -\bar{e}_1\bar{e}_2\bar{\rho}V_3\end{gathered} \tag{25}$$

$$\varphi(\xi_1,\xi_2,F) = \varphi(\xi_1,\xi_2,0) + \frac{\alpha^*}{2\xi_1}\frac{\bar{e}_1}{\bar{e}_2}\int_0^F\frac{\bar{v}_2}{\bar{v}_1}dF = \varphi(\xi_1,\xi_2,0) + 0(1 - m) \simeq \varphi(\xi_1,\xi_2,0)$$

It should be emphasized that, to the present approximation, the stream function φ in the outer region depends only on ξ_1 and ξ_2 but not on ξ_3 or F [see Eq. (25)]. The boundary conditions associated with the inner Eqs. (18–20) are, for an impermeable surface,

$$\xi_3 = 0, \qquad V_j^{(i)} = \bar{v}_{je} \text{ for } j = 1,2, \ H_0^{(i)} = H_{0w} \tag{26a}$$

$$\xi_3 \to \infty, \quad V_j^{(i)} \text{ matches } V_j^{(o)} \text{ for } j = 1,2,\S \quad H_0^{(i)} \text{ matches } H_0^{(o)} \tag{26b}$$

where superscripts (i) and (o) denote inner and outer solutions, respectively. The boundary conditions associated with the outer Eqs. (21–23) are

$$F \to 0 \quad V_j^{(o)} \text{ matches } V_j^{(i)} \text{ for } j = 1,2,$$

$$V_3^{(0)} \to -\left(\frac{2\xi_1}{\bar{e}_1\bar{e}_2\bar{\rho}^{(o)}}\right)\left(\frac{\partial\varphi}{\partial\xi_2}\right) = \left(\frac{\alpha^*}{\bar{e}_1\bar{e}_2\bar{\rho}^{(o)}}\right)\frac{\partial}{\partial\xi_2}\left(\bar{e}_1\bar{e}_3\int_0^\infty\bar{\rho}^{(i)}V_2^{(i)}d\xi_3\right) \tag{27a}$$

$$H_0^{(o)} \text{ matches } H_0^{(i)}$$

$$F \to \infty, \quad V_j^{(o)} \to 0 \text{ for } j = 1,2, \quad H_0^{(o)} \to 0 \tag{27b}$$

Although the matching conditions remain to be specified, it is of interest at this point to examine the inner and outer equations and boundary conditions with a view to the different

‡ A linear viscosity-temperature relation is assumed in what follows.

§ The quantitative statement of the matching conditions is presented in subsequent paragraphs.

interplay of streamwise flow and cross-flow in the two regions, and the consistent formulation of inner and outer solutions. The inner Eqs. (18–20) show that, in accord with the physical arguments advanced at the beginning of this section, the flow in the inner region is dominated by the effect of pressure and viscous transports. The streamwise and cross-flow velocities are coupled only through the energy equation and the temperature dependence of the viscosity. Since the flow is described by ordinary differential equations, the solutions satisfy local similarity. Specifically, in view of the boundary and matching conditions, Eqs. (26a,b), and of the relation $\bar{v}_1 \gg \bar{v}_2$ in the region of matching ($\xi_3 \to \infty$), the solutions for V_1 and H_0 exhibit the anticipated Couette-like behavior, while the solution for V_2 possesses the anticipated Poiseuille-like behavior.

For the outer region, described by the Eqs. (21–23) with the boundary conditions (27a,b) the interplay between cross-flow and streamwise flow is embodied in the boundary condition (27a) for $V_3^{(o)}$. Except for this injection-like (or suction-like) effect, due to the integral mass flow spillage in the inner region, the streamwise and cross-flow velocities in the outer region are uncoupled and amenable to sequential determination since the governing equations are linear. The formal uncoupling reflects the anticipated presence of a small cross-flow in the outer region, where the momentum flux per unit area is comparable to that in the inviscid external flow. However, the outer solutions remain linearly dependent on the a priori unknown boundary value of $V_3^{(o)}(0)$. The magnitude of this parameter, and, therefore, the dependence of the flow upon three-dimensional effects, can only be unfolded upon matching of the inner and outer solutions, and upon definition of the composite solutions. In spite of the formal similarities with a small cross-flow approximation in the outer region, the two-layer model thus retains three-dimensional effects reflected quantitatively in the dependence of the outer solutions upon the boundary condition (27a). This synthetic representation of the three-dimensional effect constitutes one of the salient results of the model; its validity is supported by the successful comparisons with "exact" solutions for wall skin friction and heat transfer as well as for streamwise and cross-flow velocity profiles reported in Sec. 6.

The two layer model also leads to a specific definition of the domains of dependence and/or influence to be considered in numerical analyses of three-dimensional boundary layers.[7] According to the model, the question is only relevant in the outer region, where the flow is described by partial differential equations. The formal uncoupling of the outer equations for streamwise flow and cross-flow identifies the domains of dependence and/or influence with streamtubes bound by inviscid flow streamlines. However, different streamtubes may not be analyzed independently of each other; the dependence of $V_3^{(o)}(0)$ upon $(\partial\varphi/\partial\xi_2)_{F\to 0}$ in Eq. (27a) requires simultaneous determination of the entire boundary-layer flow upstream of a considered station ξ_1 = constant. Thus, the process of analysis associated with the two layer model retains distinctly three-dimensional features. The point of view is again supported by the comparisons presented in Sec. 6.

The complete definition of inner and outer solutions is contingent with the stipulation of matching criteria [see Eqs. (26b) and (27a)]. These criteria must be predicated on, and be consistent with, the process whereby inner and outer equations have been derived. In this context, it is of interest to reiterate that the two layer model is of a heuristic rather than a rigorous nature; conceptually, it belongs with the second group of approximations recognized in the introduction. Indeed, any dependence on the single small parameter $(1 - m)$ can be filtered out of the full Eqs. (8–11) by a density transformation of the ξ_3 coordinate and a simultaneous asymptotic treatment of the pressure gradient parameter, viz. introduction of $\hat{\beta} = \beta^*(1 - m)^{-1}$. Under these conditions the approximate equations and their solutions cannot be recovered as the leading terms in a systematic asymptotic expansion in powers of $(1 - m)$; rather, they must be accepted as the result

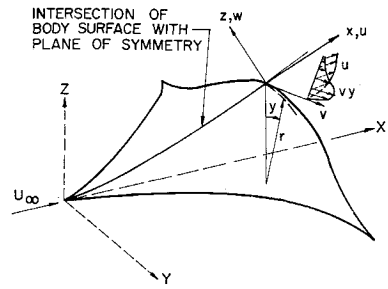

Fig. 3 Schematic diagram of flow and coordinate system for the plane of symmetry problem.

of the physical argument and order of magnitude analysis set forth above.

In the absence of a systematic asymptotic expansion framework, the matching criteria must be evolved heuristically. A review of Eqs. (15) and (16) readily shows that, if an overlap domain exists for inner and outer solutions, it must be characterized by: 1) $F \to 0$ in the outer solutions for $\bar{v}_1$ and $\bar{H}$, but $F \to F_m$ (with F_m to be defined below) in the solution for $\bar{v}_2$; and 2) $\bar{v}_1^{(i)} \to \bar{v}_{1e} = 0(1)$, $\bar{H}^{(i)} \to 1$, $\bar{v}_2^{(i)} \to \bar{v}_2$ ($\bar{v}_1^{(i)} = \bar{v}_{1e}$, $\bar{H}^{(i)} = 1$) in the inner solutions.

Distinct inner limits must be applied to the outer solutions for $\bar{v}_1$ and $\bar{H}$ and to the solution for $\bar{v}_2$ to recognize the different behavior of the streamwise and transversal momentum fluxes in the region of rapidly decreasing density.¶ In this region, the momentum flux $\bar{\rho}\bar{v}_1^2$ rapidly decreases from $0(1)$ near the outer boundary to $0(1 - m)$ near the inner boundary, while the momentum flux $\bar{\rho}\bar{v}_1\bar{v}_2$ remains uniformly $0(1 - m)$; thus, the convective terms should be retained in the equations for ξ_1-momentum and energy (in accord with the outer approximation), while they may be neglected in the equation for ξ_2-momentum (in accord with the inner approximation). Consistent with these views the overlap domain for the cross-flow is defined by

$$F \to F_m = F(\bar{v}_1^{(i)} \to \bar{v}_{1e},\ \bar{H}^{(i)} \to 1) \tag{28}$$

With the convention $F^* = 0$, for $\bar{v}_1$ and $\bar{H}$, $F^* = F_m$ for $\bar{v}_2$, and with the common notation $q^{(o)}$, $q^{(i)}$ for the outer and inner solution of $\bar{v}_1$, $\bar{v}_2$, and $\bar{H}$, the matching conditions then take the form

$$[q^{(o)}(\xi_1,\xi_2,F)]_{F\to F^*} = [q^{(i)}(\xi_1,\xi_2,F)]_{\substack{\bar{v}_1{}^i \to \bar{v}_{1e} \\ \bar{H}^i \to 1}} \tag{29}$$

The analytical statement of the two-layer model is thus completed. In the following sections the model is tested against the "exact" (numerical) similar solutions for the hypersonic laminar boundary layer near a plane of symmetry.[2]

3. Plane of Symmetry Problem and its Outer Solution

In order to facilitate the comparison with the results of Trella and Libby,[2] the two-layer model is applied to the self-similar flows near a plane of symmetry by using the coordinate system and the notation of Ref. 2, viz. (x,y,z) for the space coordinates (Fig. 3), (u,vy,w) for the corresponding components of velocity, $(\bar{u},\varphi',g)$ for the velocity and enthalpy ratios.

$$\bar{u} = u/u_e,\quad \varphi' = (1 - m)v/v_e,\quad g = H/H_e \tag{30}$$

Upon identification of the reference inviscid flow properties [ρ^*, μ^*, etc. in (7a)] with the properties along the plane of

¶ Obviously, the definition of $F_m \neq 0$ could be replaced by analysis of a third layer characterized by different magnitudes of streamwise and transversal momentum fluxes.

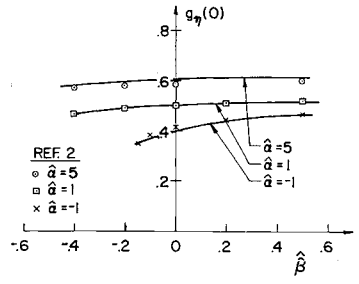

Fig. 4 Variation of wall heat-transfer parameter.

symmetry streamline, and upon density transformation, the independent variables defined in Eq. (7a) become identical to those of Ref. 2, namely

$$s = \xi_1 \qquad \eta = \int_0^{\xi_3} \bar{\rho} d\xi_3 \tag{31}$$

The governing Eqs. (8–11), specialized to similar flows with zero wall enthalpy, then become

$$-\eta\bar{u}_\eta + \bar{w}_\eta + \hat{\alpha}\varphi' = 0 \tag{32}$$

$$(\eta\bar{u} - \bar{w})\bar{u}_\eta + \hat{\beta}(g - \bar{u}^2) + \bar{u}_{\eta\eta} = 0 \tag{33}$$

$$(\eta\bar{u} - \bar{w})\varphi_\eta' + [\hat{\gamma} + (1 - m)\hat{\alpha}][g - m\bar{u}^2] - \hat{\gamma}\bar{u}\varphi' - \hat{\alpha}\varphi'^2 + \varphi_{\eta\eta}' = 0 \tag{34}$$

$$(\eta\bar{u} - \bar{w})g_\eta + g_{\eta\eta} = 0 \tag{35}$$

where

$$\bar{w} = (2s)^{1/2}\rho[(w/\rho_e\mu_e u_e r^j) - ur^j(\partial z/\partial s)] \tag{36}$$

$$\hat{\alpha} = [2sv_e]/[(1 - m)\rho_e\mu_e u_e^2 r^{3j}] \tag{37a}$$

$$\hat{\beta} = [2s(du_e/ds)]/[(1 - m)u_e] \tag{37b}$$

$$\hat{\gamma} = [2s/(r^j v_e)][d(r^j v_e)/ds] \tag{37c}$$

and a subscript η denotes derivatives with respect to η. The boundary conditions are

$$\begin{gathered}\eta = 0,\ \bar{u} = \varphi' = g = 0 \\ \eta \to \infty,\ \bar{u} \to 1,\ \varphi' \to (1 - m),\quad g \to 1\end{gathered} \tag{38}$$

The continuity Eq. (32) is identically satisfied by introducing the stream functions F and φ [see Eq. (14)]

$$F = \int_0^\eta \bar{u} d\eta \qquad \varphi = \int_0^\eta \varphi' d\eta \tag{39}$$

to obtain

$$\bar{w} = \eta\bar{u} - F - \hat{\alpha}\varphi \tag{40}$$

In accord with the discussion of Sec. 2, the three-dimensional effect is then reflected by the parametric dependence of the outer solutions upon the magnitude of $\bar{w}^{(o)}$ in the overlap domain ($F \to 0$), viz. $\bar{w}^{(o)}(0) = -\hat{\alpha}\varphi^{(o)}$, where $\varphi^{(o)}$ denotes the constant value of φ in the outer region. The particular statement of the outer Eqs. (21–23) for the plane of symmetry problem may now be obtained. In terms of the independent variable

$$f = F + \hat{\alpha}\varphi^{(o)} \tag{41}$$

and of the dependent variables

$$\nu = (1 - \bar{u}^2),\ \Phi' = \varphi' - (1 - m),\ G = (1 - g) \tag{42}$$

these equations are, for $(1 - m) \to 0$,

$$G_{ff} + fG_f = 0 \tag{43}$$

$$\nu_{ff} + f\nu_f - 2\hat{\beta}\nu = -2\hat{\beta}G \tag{44}$$

$$\Phi_{ff}' + f\Phi_f' - \hat{\gamma}\Phi = \hat{\gamma}(G - \nu) \tag{45}$$

The linear Eqs. (43–45) may be solved sequentially in closed form. The solutions satisfying the boundary conditions

$$f \to \infty, G \to 0, \nu \to 0, \Phi' \to 0 \tag{46}$$

can be expressed in terms of well-known special functions, namely

$$G(f) = -C_1(\pi/2)^{1/2}\,\mathrm{erfc}(f/2^{1/2}) \tag{47}$$

$$\nu(f) = \exp\left(-\frac{f^2}{2}\right)\left\{C_2 U\left(\frac{1}{2} + \hat{\beta}, \frac{1}{2}, \frac{f^2}{2}\right) - \frac{C_1}{2}\Gamma\left(\frac{1}{2} + \hat{\beta}\right) f\,\mathrm{erfc}\left(\frac{f}{2^{1/2}}\right)\left[M\left(\frac{1}{2} + \hat{\beta}, \frac{1}{2}, \frac{f^2}{2}\right) \times U\left(\frac{1}{2} + \hat{\beta}, \frac{3}{2}, \frac{f^2}{2}\right) + 2\hat{\beta}M\left(\frac{1}{2} + \hat{\beta}, \frac{3}{2}, \frac{f^2}{2}\right) \times U\left(\frac{1}{2} + \hat{\beta}, \frac{1}{2}, \frac{f^2}{2}\right)\right]\right\} \tag{48}$$

$$\Phi'(f) = C_3 \exp\left(-\frac{f^2}{2}\right) U\left(\frac{\hat{\gamma} + 1}{2}, \frac{1}{2}, \frac{f^2}{2}\right) + [\hat{\gamma}/(\hat{\gamma} - 2\hat{\beta})][\nu(f) - G(f)] \tag{49}**$$

where C_1, C_2, and C_3 are arbitrary constants to be determined upon matching with the inner solutions, $\mathrm{erfc}(x)$ denotes the standard complementary error function, $\Gamma(x)$ the Gamma function, $M(a,b,x)$ and $U(a,b,x)$ the Kummer's confluent hypergeometric functions.[13]

In the presumed overlap domain ($f \to \hat{\alpha}\varphi^{(o)}$) the solutions (47) and (48) behave like

$$[G(F)]_{F\to 0} \approx -C_1\left[\left(\frac{\pi}{2}\right)^{1/2}\mathrm{erfc}\left(\frac{\hat{\alpha}\varphi^{(o)}}{2^{1/2}}\right) - F\exp\left(-\frac{\hat{\alpha}^2\varphi^{(o)2}}{2}\right) + 0(F^2)\right] \tag{50}$$

$$[\nu(F)]_{F\to 0} \approx [a_1^{(0)}(\hat{\beta},\hat{\alpha}\varphi^{(o)})C_1 + a_2^{(0)}(\hat{\beta},\hat{\alpha}\varphi^{(o)})C_2] + [a_1^{(1)}(\hat{\beta},\hat{\alpha}\varphi^{(o)})C_1 + a_2^{(1)}(\hat{\beta},\hat{\alpha}\varphi^{(o)})C_2]F + 0(F^2) \tag{51}$$

$a_2^{(j)}(\hat{\beta},\hat{\alpha}\varphi^{(o)})$ being parameters defined in Appendix A. Equations (50) and (51) provide the asymptotic approximations to be used in the matching of streamwise velocity and stagnation enthalpy. The asymptotic approximation for the cross-flow as $F \to F^* \neq 0$, i.e., $f \to f^* = F^* + \hat{\alpha}\varphi^{(o)}$, is obtained from the Taylor series expansion

$$\Phi'(f) = \left[\Phi'(f^*) - \nu(f^*)\frac{\Phi_f'(f^*)}{\nu_f(f^*)}\right] + \frac{\Phi_f'(f^*)}{\nu_f(f^*)}\nu(f) + 0\{[\nu(f) - \nu(f^*)]^2\} \tag{52}$$

with $\Phi'(f^*)$ evaluated from Eq. (49), and the derivatives $\Phi_f'(f^*)$, $\nu_f(f^*)$ evaluated by straightforward differentiation of Eqs. (48) and (49).

4. Inner Solution for the Plane of Symmetry Problem

In the notation of Ref. 2, the inner equations are

$$g_{\eta\eta} = 0 \tag{53}$$

$$\bar{u}_{\eta\eta} + \hat{\beta}(g - \bar{u}^2) = 0 \tag{54}$$

$$\varphi_{\eta\eta}' + \hat{\gamma}(g - \bar{u}^2) = 0 \tag{55}$$

These are to be integrated subject to the boundary conditions

$$\eta = 0,\quad g = \bar{u} = \varphi' = 0 \tag{56}$$

and to the matching condition (29).

** The solution (49) fails when $\hat{\gamma} = 2\hat{\beta}$. Under those conditions the solution (A1) of Appendix A should be used for $\Phi'(f)$.

For $\hat{\beta} = 0$ the integrals are straightforward

$$g = \bar{u} = D_1\eta \tag{57}$$

$$\varphi' = D_3\eta - \hat{\gamma}D_1(\eta^3/6)[1 - D_1\eta/2] \tag{58}$$

with the arbitrary constants D_1 and D_3 to be determined upon matching of inner and outer solutions.

For $\hat{\beta} \neq 0$, $g_w \neq 1$, Eq. (54) is nonlinear and not amenable to an exact closed form solution. However, an approximation satisfactory for present purposes can be extracted by examining the behavior of the solution for $\eta \ll 1$, viz.

$$\bar{u}(\eta) = D_2\eta + 0(\eta^2) = D_2\eta + 0(F)$$

Since $F \to 0$ in the inner region and in the overlap domain according to the two-layer model, one may consistently approximate the integrals of Eqs. (53–55) by

$$g(\eta) = D_1\eta \tag{59}$$

$$\bar{u}(\eta) = D_2\eta \tag{60}$$

$$\varphi'(\eta) = D_3\eta - \hat{\gamma}\frac{\eta^3}{6}\left(D_1 - \frac{D_2^2\eta}{2}\right) = \frac{\bar{u}}{D_2}\left[D_3 - \frac{\hat{\gamma}}{6}\frac{\bar{u}^2}{D_2}\left(\frac{D_1}{D_2} - \frac{\bar{u}}{2}\right)\right] \tag{61}$$

with $D_1 \neq D_2$ for $\hat{\beta} \neq 0$. Within this approximation the stream functions F and $\varphi^{(o)}$ are given by

$$F = \bar{u}^2/2D_2,\ F_m = 1/2D_2 \tag{62}$$

$$\varphi^{(o)} = \frac{1}{D_2}\int_0^1 \varphi'(\bar{u})d\bar{u} = \frac{1}{2D_2^2}\left[D_3 - \frac{\hat{\gamma}}{6D_2}\left(\frac{D_1}{2D_2} - \frac{1}{5}\right)\right] \tag{63}$$

5. Composite Solution for the Plane of Symmetry Problem

In accord with the results and discussion of Sec. 2, the cross-flow φ' influences the streamwise velocity $\bar{u}$ and the stagnation enthalpy g only through the presence of the parameter $(\hat{\alpha}\varphi^{(o)})$ in the outer equations and solutions. For each value of this parameter, outer and inner solutions for $\bar{u}$ and g can be defined uniquely and matched without a detailed knowledge of φ'. However, analysis of the cross-flow is required to unfold the stream function $\varphi^{(o)}$ and, therefore, the parameter $\hat{\alpha}$ characteristic of the inviscid flow for the problem at hand. In line with these considerations, the developments for streamwise velocity and stagnation enthalpy are presented first below.

For the purpose of matching, outer and inner solutions must be cast in terms of the same independent variable, e.g., the space coordinate ξ_3 defined by

$$(1 - m)\xi_3 = \int_0^F (\nu - G)dF \tag{64a}$$

in the outer region, and by

$$(1 - m)\xi_3 = \int_0^\eta (g - \bar{u}^2)d\eta \tag{64b}$$

in the inner region. Equations (50, 51, and 64a) readily yield

$$(1 - m)\xi_3 = \{[a_1^{(0)} + (\pi/2)^{1/2}\,\mathrm{erfc}(\hat{\alpha}\varphi^{(o)}/2^{1/2})]C_1 + a_2^{(0)}C_2\}F + 0(F^2) \tag{65a}$$

as $F \to 0$ in the outer region, while Eqs. (59, 60, and 64b) give

$$(1 - m)\xi_3 = \left(\frac{g^2}{2D_1}\right) - \left(\frac{\bar{u}^3}{3D_2}\right) \tag{65b}$$

in the inner region. Equation (65b), recast in outer variables

$$(1 - m)\xi_3 = \frac{1}{2D_1}(1 - G)^2 - \left(\frac{1}{3D_2}\right)\left[1 - \left(\frac{\nu}{2}\right)\right]^3 \tag{66}$$

approximated by a three-term expansion††

$$(1 - m)\xi_3 = \left(\frac{1}{2D_1} - \frac{1}{3D_2}\right) + \left(\frac{\nu}{2D_2} - \frac{G}{D_1}\right) - \left(\frac{\nu^2}{4D_2} - \frac{G^2}{2D_1}\right) \tag{67}$$

and combined with Eqs. (50) and (51) is then compared with Eq. (65a); term by term matching results in two equations for the unknown constants C_1, C_2, D_1, and D_2, namely

$$\frac{D_1}{2}[a_1^{(0)}C_1 + a_2^{(0)}C_2]\left[1 - \frac{a_1^{(0)}}{2}C_1 - \frac{a_2^{(0)}}{2}C_2\right] + \left(\frac{\pi}{8}\right)^{1/2}C_1D_2\,\mathrm{erfc}\left(\frac{\hat{\alpha}\varphi^{(o)}}{2^{1/2}}\right)\left[2 + \left(\frac{\pi}{2}\right)^{1/2} \times C_1\,\mathrm{erfc}\left(\frac{\hat{\alpha}\varphi^{(o)}}{2^{1/2}}\right)\right] = \left(\frac{D_1}{3} - \frac{D_2}{2}\right) \tag{68a}$$

$$D_1[a_1^{(0)}C_1 + a_2^{(0)}C_2]\left[D_2 + \frac{a_1^{(0)}}{2}C_1 - \frac{a_2^{(0)}}{2}C_2\right] + \left(\frac{\pi}{2}\right)^{1/2}C_1D_2\,\mathrm{erfc}\left(\frac{\hat{\alpha}\varphi^{(o)}}{2^{1/2}}\right)\left[D_1 + C_1\exp\left(-\frac{\hat{\alpha}^2\varphi^{(o)2}}{2}\right)\right] = \frac{D_1}{2}[a_1^{(1)}C_1 + a_2^{(1)}C_2] - C_1D_2\exp\left(-\frac{\hat{\alpha}^2\varphi^{(o)2}}{2}\right) \tag{68b}$$

Two additional equations arise from the requirement

$$D_2(1 - G) = D_1[1 - (\nu/2)]$$

in the overlap domain, viz., upon substitution of Eqs. (50) and (51),

$$D_2[1 + (\pi/2)^{1/2}C_1\,\mathrm{erfc}(\hat{\alpha}\varphi^{(o)}/2^{1/2})] = D_1[1 - (a_1^{(o)}/2)C_1 - (a_2^{(0)}/2)C_2] \tag{68c}$$

$$D_2C_1\exp[-(\hat{\alpha}^2\varphi^{(o)2}/2)] = D_1[(a_1^{(1)}/2)C_1 + (a_2^{(1)}/2)C_2] \tag{68d}$$

Simultaneous numerical solution of Eqs. (68a, b, c, d) yields the constants of integration and, therefore, defines the profiles in the inner and outer regions. Considerable simplification occurs in the case $\hat{\beta} = 0$ wherein (68a, b) are reduced to the form

$$C_1 = -(2/3\pi)^{1/2}[\mathrm{erfc}(\hat{\alpha}\varphi^{(o)}/2^{1/2})]^{-1} \tag{69a}$$

$$D_1 = -C_1\exp[-(\hat{\alpha}^2\varphi^{(o)2}/2)] \tag{69b}$$

An immediate test of the two layer model is obtained by specializing (69a, b) to the classical two-dimensional flat plate problem ($\varphi^{(o)} = 0$). The present analysis gives for the slope of the velocity profile at the wall $\bar{u}_\eta(0) \approx 0.46$ compared with the exact value $\bar{u}_\eta(0) = 0.47$. Thus, the matching in terms of the ξ_3 variable can provide good accuracy; the three-dimensional flow results presented in the following section further recommend this choice for general applications.

The matching of outer and inner solutions for the cross-flow can now be implemented. Substitution of Eqs. (49, 52, and 61) into Eq. (29) readily yields two linear equations in the two unknown constants of integration C_3 and D_3, namely

$$\Phi'(f^*,C_3) - [\nu(f^*)/\nu_f(f^*)]\Phi_f'(f^*,C_3) = (D_3/D_2) + \hat{\gamma}/(12D_2^2)[1 - (2D_1/D_2)] \tag{70a}$$

$$\Phi_f'(f^*,C_3)/\nu_f(f^*) = -(D_3/2D_2) - (\hat{\gamma}/6D_2^2)[1 - (3D_1/2D_2)] \tag{70b}$$

where $f^* = (1/2D_2) + \hat{\alpha}\varphi^{(o)}$. Upon solution of Eqs. (70a, b), the stream function $\varphi^{(o)}$ may be evaluated from Eq. (63) and,

†† The term $(\nu/D_2 - G/D_1)$ is identically zero for $\hat{\beta} = 0$, and is of order ν^2 for $\hat{\beta} \neq 0$.

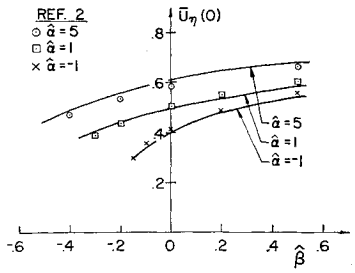

Fig. 5 Variation of streamwise wall shear parameter.

the parameter $\hat{\alpha}$, characteristic of the inviscid flow, may be unfolded from the product $\hat{\alpha}\varphi^{(o)}$.

Finally, composite solutions may be constructed following the rules of matched asymptotic expansion techniques, viz.

$$q^{(c)}(\xi_3) = q^{(o)}(\xi_3) + q^{(i)}(\xi_3) - [q^{(o)}(\xi_3)]_{F\to F^*} \qquad (71)$$

where q denotes either G^2, ν^2, or φ' and superscripts (c), (i), (o) identify composite, inner and outer solutions, respectively. As an example, the details of constructing Eq. (71) are presented here for $q = \nu^2$. First, a value of f is chosen and $\xi_3(f)$ is determined from Eq. (64a)

$$(1 - m)\xi_3(f) = \int_{\hat{\alpha}\varphi^{(o)}}^{f} (\nu - G)df$$

$G(f)$ and $\nu(f)$ being described by Eqs. (47) and (48). Then Eq. (48) itself is used to describe the outer solution

$$\nu^{(o)2} = [\nu^{(o)}(f)]^2 \qquad (72)$$

Passing to the inner solution, Eq. (65b) is rewritten in the form

$$(1 - m)\xi_3 = (D_1\bar{u}^2/2D_2^2) - (\bar{u}^3/3D_2)$$

and solved for ν^2 to obtain

$$\nu^{(i)2} = \left(1 - \left\{\frac{D_1}{D_2}\left[\frac{1}{2} + \cos\left(\frac{\theta}{3}\right)\right]\right\}^2\right)^2 \qquad (73a)$$

with

$$\theta = \pi + \cos^{-1}\left[\frac{12D_2^4}{D_1^3}(1 - m)\xi_3 - 1\right] \qquad (73b)$$

Finally the inner limit of the outer solution is derived from Eqs. (51) and (65a), viz.

$$[\nu^2(\xi_3)]_{F\to 0} = [a_1^{(0)}C_1 + a_2^{(0)}C_2]^2 + \left\{\frac{2(a_1^{(0)}C_1 + a_2^{(0)}C_2)(a_1^{(1)}C_1 + a_2^{(1)}C_2)}{\left[a_1^{(0)} + \left(\frac{\pi}{2}\right)^{1/2}\operatorname{erfc}\left(\frac{\hat{\alpha}\varphi^{(o)}}{2^{1/2}}\right)\right]C_1 + a_2^{(0)}C_2}\right\}(1 - m)\xi_3 \qquad (74)$$

The analytical statement of the two-layer model is thus completed; the assessment against known exact solutions may now be undertaken.

6. Results and Discussions

The two-layer model and the associated solutions (see Secs. 3, 4, and 5) reduce the analysis of self-preserving hypersonic laminar boundary layers near a plane of symmetry to a rapid exercise in algebra, specifically the determination of the constants of integration and the construction of the composite solutions (see Sec. 5). A comparison between the predictions of the model and the exact results obtained by numerical integration of the full boundary-layer equations[2] provides a comprehensive test on the range of applicability of the model; indeed, the considered family of flows encompasses a broad variety of situations covering the spectrum from favorable to adverse streamwise pressure gradients, and from large outflow to large inflow in the transversal direction.

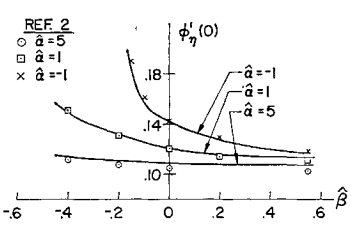

Fig. 6 Variation of cross-flow shear parameter.

The wall heat-transfer parameter, the streamwise shear parameter and the cross-flow shear parameter predicted by the two-layer model for a number of cases are compared in Figs. 4, 5, and 6 with the results of Ref. 2. The comparison is quite favorable. The percent differences between approximate and "exact" results do not exceed 5% over the entire range of conditions considered; their magnitude is essentially independent of the streamwise pressure gradient parameter $\hat{\beta}$ at fixed cross-flow parameter $\hat{\alpha}$, and is only mildly sensitive to changes in $\hat{\alpha}$ at fixed $\hat{\beta}$ [it becomes largest ($\approx$5%) for the largest outflows considered]. The insensitivity to $\hat{\beta}$ indicates that the inertial forces remain negligible in the inner region even in the presence of large adverse pressure gradients; however, the behavior under conditions approaching separation remains outside the range investigated here and in Ref. 2.

The good agreement in shear and heat transfer parameters is also reflected in the velocity and enthalpy profiles; a representative comparison between the present predictions and those of Ref. 2 is exhibited in Fig. 7.

The apparent success of the two-layer model elicits further inquiries about its essential aspects; among these are a) how closely do the composite solutions follow a structural subdivision into inner and outer region? b) how realistic is the crudest physical model[8] where the outer region is approximated by a solid plate that drives and confines the inner region into a Couette-like streamwise motion and a Poiseuille-like cross-flow motion? Some insights are obtained by inspection of typical graphs of inner, outer, and composite solutions (Fig. 8). The structural subdivision is validated by the close agreement between the actual composite solutions and the locally appropriate (either inner or outer) approximate solutions; transitions from inner to outer behavior occurs rapidly in a narrow intermediate region [about $(1 - m)\xi_3 \approx 0.37$ in the figure]. The crude physical model is corroborated by a juxtaposition of the inner solutions for streamwise and cross-flow velocities; in this view it is clear that both solutions are essentially consistent with the presence of a fictitious plate moving at $\bar{u} = 1$.‡‡ In principle, the separate balances of streamwise and transversal momentum would require consideration of two distinct, albeit adjacent, plates, each constraining the motion in one direction; however, the small slip of the cross-flow relative to the fictitious plate moving with $\bar{u} = 1$ (Fig. 8) indicates that a single plate model may suffice for a preliminary analysis. Within this approximation Eq. (61) leads to a

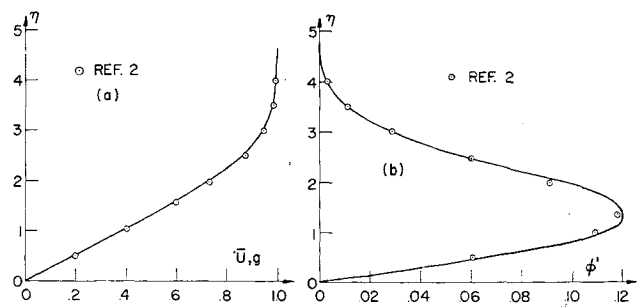

Fig. 7 Velocity and stagnation enthalpy profiles. a) Streamwise velocity and stagnation enthalpy. b) Cross-flow velocity.

‡‡ In the absence of matching the position of the plate can be determined by applying integral momentum considerations to the flow in the inner region.[8]

simple expression for the cross-flow shear parameter in terms of the streamwise shear parameter, the heat-transfer parameter and the transversal pressure gradient parameter $\hat{\gamma}$

$$\varphi_\eta'(0) = D_3 = \frac{\hat{\gamma}}{6D_2}\left[\frac{D_1}{D_2} - \frac{1}{2}\right] \tag{75}$$

The practical usefulness of Eq. (75) is demonstrated by a comparison with exact results[2] (Fig. 9); this shows that the qualitative trends are well reproduced, although with lesser accuracy than is accrued by the composite solution shown in Fig. 6. It is of interest to note that the relation Eq. (75) has been derived by considerations restricted to the inner region where local similarity is always satisfied;§§ accordingly, Eq. (75) is applicable not only to the similar flows considered here but to nonsimilar boundary layers as well.

A final comment is in order with regard to the extension of the two-layer model for application at moderate (nonhypersonic) Mach numbers. As noted in previous sections, the model is not contingent with a singular dependence of the full boundary-layer equations upon a Mach number parameter; in fact, any essential Mach number dependence is filtered out by a density transformation of the ξ_3-coordinate. The outer and inner equations must then be viewed as approximations to the full equations in density transformed coordinates; as such they must be effective at all Mach numbers. The strong conclusion is reconciled with the hypersonic-oriented heuristic derivation of the model [the order of magnitude estimates Eqs. (15) and (16) are appropriate to hypersonic flows] if the existence of two regions characterized by widely different momentum fluxes per unit area is recognized for all Mach numbers. Two such regions always exist; their description and matching in density transformed coordinated are obviously independent of Mach number. Thus, the hypersonic-oriented approach has served the function of identifying the approximations appropriate to the two regions and the criteria for matching; the density transformation insures the validity of the approximation at all Mach numbers.

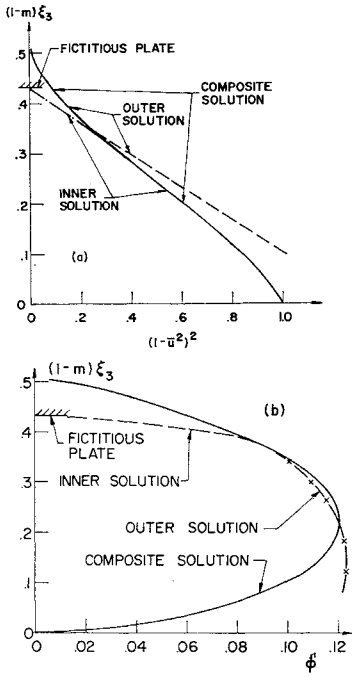

Fig. 8 Juxtaposition of inner, outer, and composite solutions: a) Streamwise velocity, b) Cross-flow velocity.

§§ It may be of interest to note the analogy between the present model and the classical subdivision of a turbulent boundary layer into a wall region and a wake region. In both cases, the inner region is in local equilibrium, while the outer region carries the memory of flow history.

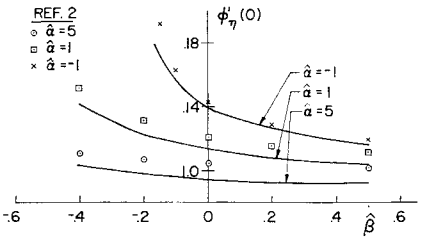

Fig. 9 Variation of cross-flow shear parameter predicted by Poiseuille flow approximation.

In conclusion, the positive aspects of the two layer approach, admittedly heuristic and approximate, are associated with physical insights and analytical simplifications; among these: 1) the wall injection model for the interaction between streamwise flow and cross-flow in the outer region; 2) the reduction of the outer equations to linear form with attendant benefits of comparatively rapid and straightforward solution (in closed form); and 3) the local similarity model for the inner region with consequent simplification of the equations to ordinary differential form. In view of these aspects, of the satisfactory results obtained for the broad class of hypersonic plane of symmetry problems, and of the essential Mach number independence of the solutions in density transformed coordinates, it is concluded that the two-layer model can provide a useful basis for extensive analysis and understanding of three-dimensional boundary-layer problems.

Appendix A

For $2\hat{\beta} = \hat{\gamma}$ the solution (49) for the cross-flow $\Phi'(f)$ in the outer region must be replaced by

$$\Phi' = \exp\left(-\frac{f^2}{2}\right)\left\{C_3 U\left(\frac{\hat{\gamma}+1}{2}, \frac{1}{2}, \frac{f^2}{2}\right) + \frac{C_1}{2}\Gamma\left(\frac{\hat{\gamma}+1}{2}\right) f \operatorname{erfc}\left(\frac{f}{2^{1/2}}\right)\left[M\left(\frac{\hat{\gamma}+1}{2}, \frac{1}{2}, \frac{f^2}{2}\right) \times U\left(\frac{\hat{\gamma}+1}{2}, \frac{3}{2}, \frac{f^2}{2}\right) + \hat{\gamma} M\left(\frac{\hat{\gamma}+1}{2}, \frac{3}{2}, \frac{f^2}{2}\right) \times U\left(\frac{\hat{\gamma}+1}{2}, \frac{1}{2}, \frac{f^2}{2}\right)\right] + \hat{\gamma}\left(\frac{1}{2\pi}\right)^{1/2} \Gamma\left(\frac{\hat{\gamma}+1}{2}\right) \times \left[M\left(\frac{\hat{\gamma}+1}{2}, \frac{1}{2}, \frac{f^2}{2}\right) \int_f^\infty U\left(\frac{\hat{\gamma}+1}{2}, \frac{1}{2}, \frac{f^2}{2}\right) \nu(f) df + U\left(\frac{\hat{\gamma}+1}{2}, \frac{1}{2}, \frac{f^2}{2}\right) \int_{\hat{\alpha}\varphi^{(o)}}^f M\left(\frac{\hat{\gamma}+1}{2}, \frac{1}{2}, \frac{f^2}{2}\right) \nu(f) df\right]\right\} \tag{A1}$$

The solution (A1) is valid for all $\hat{\beta}$ and $\hat{\gamma}$; Eq. (49) was indicated in the main text because of its greater simplicity.

The parameters $a_i^{(j)}(\hat{\beta}, \hat{\alpha}\varphi^{(o)})$ introduced in Eq. (51) are defined by

$$a_1^{(0)} = -\left[\Gamma\left(\frac{1}{2} + \hat{\beta}\right) \times \hat{\alpha}\varphi^{(o)} \operatorname{erfc}\left(\frac{\hat{\alpha}\varphi^{(o)}}{2^{1/2}}\right)\right] \exp\left(-\frac{\hat{\alpha}^2\varphi^{(o)2}}{2}\right) A \tag{A2}$$

$$a_2^{(0)} = U[\tfrac{1}{2} + \hat{\beta}, \tfrac{1}{2}, (\hat{\alpha}^2\varphi^{(o)2}/2)] \exp(-\hat{\alpha}^2\varphi^{(o)2}/2) \tag{A3}$$

$$a_1^{(1)} = -a_1^{(0)}\left\{\hat{\alpha}\varphi^{(o)}\left(1 - \frac{B}{A}\right) - \frac{1}{\hat{\alpha}\varphi^{(o)}} + \left(\frac{2}{\pi}\right)^{1/2} \exp\left(-\frac{\hat{\alpha}^2\varphi^{(o)2}}{2}\right)\left[\operatorname{erfc}\left(\frac{\hat{\alpha}\varphi^{(o)}}{2^{1/2}}\right)\right]^{-1}\right\} \tag{A4}$$

$$a_2^{(1)} = -\hat{\alpha}\varphi^{(o)}\left[a_2^{(0)} + \left(\frac{1}{2}+\hat{\beta}\right)\times U\left(\frac{3}{2}+\hat{\beta},\frac{3}{2},\frac{\hat{\alpha}^2\varphi^{(o)2}}{2}\right)\exp\left(-\frac{\hat{\alpha}^2\varphi^{(o)2}}{2}\right)\right] \quad \text{(A5)}$$

where

$$A(\hat{\beta},\hat{\alpha}\varphi^{(o)}) = \frac{1}{2}M\left(\frac{1}{2}+\hat{\beta},\frac{1}{2},\frac{\hat{\alpha}^2\varphi^{(o)2}}{2}\right)\times U\left(\frac{1}{2}+\hat{\beta},\frac{3}{2},\frac{\hat{\alpha}^2\varphi^{(o)2}}{2}\right) + \hat{\beta}U\left(\frac{1}{2}+\hat{\beta},\frac{1}{2},\frac{\hat{\alpha}\varphi^{(o)2}}{2}\right)\times M\left(\frac{1}{2}+\hat{\beta},\frac{3}{2},\frac{\hat{\alpha}^2\varphi^{(o)2}}{2}\right) \quad \text{(A6)}$$

$$B(\hat{\beta},\hat{\alpha}\varphi^{(o)}) = \frac{1}{2}\left[(1+2\hat{\beta})M\left(\frac{3}{2}+\hat{\beta},\frac{3}{2},\frac{\hat{\alpha}^2\varphi^{(o)2}}{2}\right)\times U\left(\frac{1}{2}+\hat{\beta},\frac{3}{2},\frac{\hat{\alpha}^2\varphi^{(o)2}}{2}\right) - \left(\frac{1}{2}+\hat{\beta}\right)\times U\left(\frac{3}{2}+\hat{\beta},\frac{5}{2},\frac{\hat{\alpha}^2\varphi^{(o)2}}{2}\right)\cdot M\left(\frac{1}{2}+\hat{\beta},\frac{1}{2},\frac{\hat{\alpha}^2\varphi^{(o)2}}{2}\right)\right] + \beta\left[\left(\frac{1+2\hat{\beta}}{3}\right)U\left(\frac{1}{2}+\hat{\beta},\frac{1}{2},\frac{\hat{\alpha}^2\varphi^{(o)2}}{2}\right)\times M\left(\frac{3}{2}+\hat{\beta},\frac{5}{2},\frac{\hat{\alpha}^2\varphi^{(o)2}}{2}\right) - \left(\frac{1}{2}+\hat{\beta}\right)\times U\left(\frac{3}{2}+\hat{\beta},\frac{3}{2},\frac{\hat{\alpha}^2\varphi^{(o)2}}{2}\right)M\left(\frac{1}{2}+\hat{\beta},\frac{3}{2}\frac{\hat{\alpha}^2\varphi^{(o)2}}{2}\right)\right] \quad \text{(A7)}$$

References

[1] Cheng, H. K., "The Shock Layer Concept and Three-Dimensional Hypersonic Boundary Layers," Rept. AF-1285-A-3, Jan. 1961, Cornell Aeronautical Labs., Buffalo, N. Y..

[2] Trella, M. and Libby, P. A., "Similar Solutions for the Hypersonic Laminar Boundary Layer Near a Plane of Symmetry," *AIAA Journal*, Vol. 3, No. 1, Jan. 1965, pp. 75–83.

[3] Vaglio-Laurin, R., "Laminar Heat Transfer on Three-Dimensional Blunt Nosed Bodies in Hypersonic Flow," *ARS Journal*, Vol. 29, No. 2, Feb. 1959, pp. 123–129.

[4] Vaglio-Laurin, R., "Turbulent Heat Transfer on Blunt Nosed Bodies in Two-Dimensional and General Three-Dimensional Hypersonic Flow," *Journal of the Aerospace Sciences*, Vol. 27, No. 1, Jan. 1960, pp. 27–36; also TN58-301, Sept. 1958, Wright Air Development Center.

[5] Kang, S. W., Rae, W. J., and Dunn, M. G., "Effects of Mass Injection on Compressible Three-Dimensional Laminar Boundary Layers," *AIAA Journal*, Vol. 5, No. 10, Oct. 1967, pp. 1738–1745.

[6] Fannelop, T. K., "A Method of Solving the Three-Dimensional Laminar Boundary Layer Equations with Applications to a Lifting Re-entry Body," *AIAA Journal*, Vol. 6, No. 6, June 1968, pp. 1075–1084.

[7] Der, J., Jr., "A Study of General Three-Dimensional Boundary Layer Problems by an Exact Numerical Method," AIAA Paper 69-138, New York, 1969.

[8] Vaglio-Laurin, R., "Viscous Hypersonic Flow Past Slender Bodies at Incidence," Paper 25, *AGARD Conference Proceedings 30, Hypersonic Boundary Layers and Flow Fields*, May 1968.

[9] Glauert, M. B. and Lighthill, M. J., "The Axisymmetric Boundary Layer on a Long Thin Cylinder," *Proceedings of the Royal Society*, London, Ser. A, Vol. 230, No. 1181, June 1955, pp. 188–203.

[10] Stewartson, K., "Viscous Hypersonic Flow Past a Slender Cone," *The Physics of Fluids*, Vol. 7, No. 5, May 1964, pp 667–675; also see Erratam, Vol. 7, No. 12, Dec. 1964, pp. 2025–2026.

[11] Rosenhead, L., ed., *Laminar Boundary Layers*. Clarendon Press, Oxford, 1963, Ch. VI, Parts III and IV, pp. 318–331.

[12] Hayes, W. D. and Probstein, R. F., "Viscous Hypersonic Similitude," *Journal of the Aerospace Sciences*, Vol. 26, No. 12, Dec. 1959, pp. 815–824.

[13] Abromowitz, M. and Stegun, L. A., eds., *Handbook of Mathematical Functions*, National Bureau of Standards Applied Mathematical Ser. 55, June 1964.